Thakur et al., J Proteomics Bioinform 2018, 11:10
DOI: 10.4172/0974-276X.1000486

Journal of
Proteomics & Bioinformatics

Research Article Open Access

"ESI-MS-Bioinformatics Studies on Crosslinking of α A-Crystallin and Lysozyme using a New Small Aryl Azido-N-HydroxySuccinimidyl Heterobifunctional Crosslinker based on a Metabolite of the Alternative Kynurenine Pathway"

Sujeet Kumar Thakur[1], Shreya Pal[2], Ankur Kumar[3], Renu Goel[3] and Sambasivan Venkat Eswaran[1]*

[1]*Regional Centre for Biotechnology, Under the Auspices of UNESCO- DBT, (NCR Biotech Science Cluster), 3rd Milestone, Faridabad-Gurgaon Expressway, Faridabad-121001, Haryana, India*
[2]*Amity University Haryana, Amity Education Valley, Gurgaon District, Manesar-122413, Haryana, India*
[3]*Drug Discovery Research Center, Translational Health Science and Technology Institute, (NCR Biotech Science Cluster), 3rd Milestone, Faridabad-Gurgaon Expressway, Faridabad-121001, Haryana, India*

Abstract

The use of a new small aryl azido-N-Hydroxysuccinimidyl heterobifunctional crosslinker for crosslinking of αA-crystallin and lysozyme is described here. The crosslinker is based on the small molecule, 3-hydroxy anthranilic acid (3HAA) a part of the kynurenine pathway in Tryptophan metabolism. Enhanced amounts of 3HAA are found in disease states in the human body. The new crosslinker contains a photo labile azido group and an amine reactive, N-hydroxy succinimide (NHS) group. Small crosslinkers capture interacting protein interfaces better, while the larger ones are more useful for identifying interacting partners. Our earlier work has shown that aryl azides in this series lead to 'long lived' transients allowing for increased intermolecular reaction rates, otherwise difficult to achieve. Using this crosslinker, successful crosslinking of αA-Crystallin & lysozyme has been demonstrated in two steps i. e. incubation followed by photolysis (366 nm, 6W UV lamp). Previous studies on αA- Crystallin have mostly used only homobifunctional crosslinkers. As hypothesized by us, the use of a heterobifunctional crosslinker has indeed led to more efficient crosslinking. This has been confirmed using SDS-PAGE, ESI-MS/MS (following trypsinization of the homo and hetero 'dimer' bands) and use of StavroX 3.6.0.1, the bioinformatics software especially suited for analyzing intermolecular crosslinking. These investigations are expected to lead to a better understanding of the role of αA-Crystallin in chaperoning mechanism and in cataractogenesis.

Keywords: 3-Hydroxyanthranilic acid; Kynurenine; ESI-MS; StavroX 3.6.0.1

Introduction

Alpha-Crystallin the transparent, heat stable, water soluble protein of the human eye lens has been studied earlier exhaustively [1]. α-Crystallin consists of αA (173 amino acids; Mw; 19909) and αB (175 amino acids; Mw; 20159), "in a molar ratio which is variable among species". αA-Crystallin and αB-Crystallin play a very important role in keeping the human eye lens transparent and to prevent aggregation of these water soluble proteins leading to opaqueness and cataract. However, only very recently their role as therapeutics, for treating not only eye diseases, but also other major diseases has been demonstrated [2-9]. It is pertinent to note that even in cases of concussion of the brain, treatment with Crystallins has helped in recovery from the neurodegenerative injuries [10]. However, since Crystallins also cause diseases, it is a trade-off between their activity as possible therapeutics and simultaneously as disease causing agents, makes it necessary to tread the path with great caution. It is also known that metabolites of the alternative Kynurenine pathway (Supplementary Figure 1) of the Tryptophan catabolism have an important role in disease states. These include Huntington's disease, Parkinson's disease, HIV-AIDS, and cerebral malaria. Thus, the ratio of 3-Hydroxyanthranilic acid (3HAA) to Anthranilic acid (AA) in the human brain differentiates a patient from a normal person [11]. 3-Hydroxykynurenine (3HK) and 3HAA oxidize α A-Crystallin, which leads to the production of hydrogen peroxide in the human eye and has been implicated in cataractogensis [12]. Earlier work has shown that 3HK and 3HAA reduce Cu (II) and Fe (III) and generate superoxide and H2O2, when the kynurenine pathway is activated, which could be relevant in Cataractogenesis. These workers [13] even carried out cyclic voltammetry studies showing loss of Cu (II) by complexation and/reduction with 3HAA being the most effective. Srivastava et al. [14,15] have carried out mass spectral studies of the proteins of human eye lens and correlated it with age; larger number of proteins being found with increasing age. The D. Balasubramanian group at the L.V Prasad Eye Hospital, Hyderabad, India [16,17] has done pioneering work on crystallins. For example, these workers showed that transglutaminase mediated dimerization of alpha Crystallin decreases its chaperone like activity with considerable loss of tertiary structure and decrease in its secondary structure based fluorescence. The effect of alpha Crystallin on the refolding of the denatured-disulphide intact and denatured-lysozyme was studied. However, "no refolding of disulphide intact enzyme occurred but alpha crystallin inhibited the aggregation and

***Corresponding author:** Sambasivan Venkat Eswaran, Regional Centre for Biotechnology, Under the Auspices of UNESCO- DBT, (NCR Biotech Science Cluster), 3rd Milestone, Faridabad-Gurgaon Expressway, Faridabad-121001, Haryana, India, Tel: +001292848888; E-mail: samba.eswaran@rcb.res.in

Received October 24, 2018; **Accepted** November 08, 2018; **Published** November 15, 2018

Citation: Thakur SK, Pal S, Kumar A, Goel R, Eswaran SV (2018) "ESI-MS-Bioinformatics Studies on Crosslinking of αA-Crystallin and Lysozyme using a New Small Aryl Azido-N-HydroxySuccinimidyl Heterobifunctional Crosslinker based on a Metabolite of the Alternative Kynurenine Pathway". J Proteomics Bioinform 11: 192-200. doi: 10.4172/0974-276X.1000486

oxidative renaturation of denatured-reduced lysozyme" [18,19]. "Crystallin is known to prevent the heat induced aggregation of the protein by forming a stable complex" These workers chose Lysozyme as it "is one of the most extensively studied enzyme for its refolding properties". Peschek et al. [20] (a) demonstrated the chaperoning function of αA-Crystallin in binding with lysozyme, leading to soluble and insoluble proteins. These workers "studied the chaperoning activity of αA-Crystallin in aggregation assays using Lysozyme as a substrate". Saïd Abgar et al. [20] (b) studied the chaperoning function with αA-Crystallin and Lysozyme and they also stated that "we have chosen Lysozyme because many aspects of its structure have been extensively studied". Krishna Sharma's [21-24] group reported the differences between αA-WT and mutant-G98R Crystallins. Using the homobifunctional crosslinker d0/d4(1:1) deuterium labeled BS2G and used the GPMAW software to show that majority of inter subunit crosslinking was clustered in K88 region in αA-WT Crystallin, while in the mutant-G98R Crystallin, crosslinking was seen in the K99 region of the protein. Thus, in the wild type protein, crosslinking is at K88 and in the mutant it shifts to K99. This one difference, according to them reflects the different oligomerization and conformational changes in the mutant that contribute to its aggregation, making the mutant αA-Crystallin more prone to cataract formation. Their studies have helped identify the Alpha Crystallin Domain (ACD), which is common to most known HSPs. The ACD of αA-Crystallin is now referred to as the 'Mini Alpha crystallin Chaperons' ('MACs'), which is represented by the 70"KFVIFLDVKHFSP"82 sequence [25-27]. 3-D representation of MACs using protein Swiss server in αA-Crystallin where MAC (represented as a mesh shadow is shown in Supplementary Figure 2. Chaperons may work as "holdase", "foldase" and "unfoldase" functions for stabilizing the non-native/ native state to prevent protein aggregation and to make misfolded state conformations by to regain the original conformation [28].

Many crosslinkers are known in literature and are commercially available [29,30]. Thus one has moved away from the days when formaldehyde and glutaraldehyde were used as crosslinkers which brought about indiscriminate crosslinking. Nowadays, zero length, isotope labeled, MS cleavable, homo and heterobifunctional crosslinkers are known. The difficulty is how to differentiate and separate the uncrosslinked peptides from the crosslinked ones, especially when the latter are found only in low abundance. This is referred to as "a needle in the hay stack" problem. This has been overcome in recent years, by the use of strong cation exchange (SCX) chromatography which help separate or enrich the croslinked fragments (which are invariably charged) from the uncross linked fragments which are neutral. It is also known that smaller crosslinkers give better information about interacting interfaces while the larger crosslinkers give better information about the interacting sites. Progress in this field has also been possible due to great advances in the field of mass spectrometry like MALDI-MS, MS/MS, ESI-MS [31- 35], which allow detailed investigations even when the amount of sample available is very small. Similarly, great advances have happened in Bioinformatics tools like the MS3D Links, GPMAW, Xlink, Kojac, CLMS vaults, pLink, StavroX & MeroX [36-39]; the latter being especially suitable for cleavable MS. Hagan Bayley [40], had predicted that intermediates during thermolysis/photolysis of pentafluro phenyl azide could lead to efficient photo affinity labeling agents, as these involve "long- lived" transients. This was subsequently shown to be true by M S Platz et al. [41,42]. Tomioka [43] showed that such 'long-lived' transients involve "slippery potential energy surfaces" and could lead to increase intermolecular crosslinking. Computational studies by Borden et al. [44] provided the much needed theoretical basis that there is an increase in the singlet-triplet gap. We have also similarly prepared Aryl Azido-N-hydroxy succinimidyl (NHS) heterobifunctional crosslinkers based on 'long-lived' transients, which do not require any ortho-flanking fluorine atoms [45-51]. The latter is a great advantage as fluorination is both hazardous and toxic and preparation of our new crosslinker does not involve any such hazardous steps. It may be noted that aryl azides are now referred to as "green reagents" [52]. Earlier crosslinking studies on αA-Crystallin have mostly used homobifunctional crosslinkers. In the current study, a new small aryl-azido-NHS- heterobifunctional crosslinker based on 3HAA, a catabolite of Tryptophan in the Kynurenine pathway has been employed. The new crosslinker is based on 'long-lived' transients, which could promote efficient intermolecular crosslinking. Crosslinking has been done here using a two-step protocol. The first step involves incubation which is followed by photolysis (366 nm, 6W UV lamp) to crosslink αA-crystallin (19kDa) and lysozyme (14kDa). From the intermolecularly crosslinked (33kDa) band thus obtained, we have identified sites of crosslinking and characterized a previously unidentified and a most significant intermolecularly crosslinked fragment, with a very precise m/ z value. This fragment which contains fragments from both αA-Crystallin and Lysozyme provides a positive, confirmatory evidence for the binding of the two proteins. These investigations are expected to lead to a better understanding of the role of αA-Crystallin in chaperoning mechanism and cataractogenesis and for studies on other diseases, as well. This technique of chemical crosslinking-mass-spectrometry-bioinformatics is useful in proteomics, systems and structural biology, antibody drug conjugates (ADCs) and even for refining structures based on cryo– EM [53-64]. It is hoped that this new technique would be amenable to High Throughput Screening (HTS) of large number of patient samples in a rapid, reliable and routine manner.

Materials and Methods

Synthesis of the new crosslinker

The new heterobifunctional crosslinker, 2-Azido-3-Hydroxy-benzoic acid-2, 5-dioxo-pyrrolidin-1-yl ester (135 mg)**, (II)** was prepared from 2-Amino-3-Hydroxy-benzoic acid **(I)** 200 mg (1.19 mmol) was taken and dissolved in 8 ml of concentrated hydrochloric acid and 2 ml of water and cooled at 0°C, this was diazotized by slow addition of sodium nitrate (140 mg, 1.2mmol) in minimum amount of water required. A solution of sodium azide NaN3 (120 mg, 2mmol.) and sodium acetate (3.36 g, 40mmol) in minimum water was taken and slowly added to the diazotized solution, when an off white solid settled down on the bottom of the vessel. This compound was filtered and thus compound **(II)** was obtained (yield, 175 mg). 175 mg of compound **(II)** was dissolved in 10 ml of dichloromethane (DCM) and then N-hydroxy sucinimide (NHS), (59.8 mg, 0. 52 mmol) and dicyclohexyl carbodiimide (DCC) (107 mg,0.52 mmol) were added and the reaction mixture was stirred at room temperature overnight. The solution was filtered to separate the urea side product. The filtrate was distilled and put in a desiccator with P2O5 when pale white compound **(III)** was obtained Supplementary Figure 3; M.P. 182OC; MS, M+H+ 277.1 (Supplementary Figure 4).

Chemical crosslinking

Materials required:

- Freshly prepared 1M Lysozyme solution

- αA-Crystallin 1 mg/mL
- 200 M Crosslinker solution
- PBS Buffer

SDS-PAGE and in-gel digestion

The FASTA sequence for Lysozyme (Supplementary Figure 5), αA-Crystallin (Supplementary Figure 6) and for 1: 1 mixture of lysozyme and αA-Crystallin Supplementary Figure 7 are given in the supplementary material. The SDS- PAGE standard protocol used for this studies is given in Supplementary Figure 8**.** 10 micrograms of proteins were incubated with the crosslinker (overnight) and then photolyzed at (366 nm, 6W UVlamp, 30 mins.) and then resolved by SDS-PAGE (Lysozyme, αA-Crystallin and 1:1 mixture of lysozyme and αA-Crystallin Supplementary Figures 9 and 10**.** The gels were stained with Commassie blue and destained with water. Gel pieces were excised and in-gel digestion was carried out [65]. The excised bands were destained with 40 mM ammonium bicarbonate (ABC) in 40% acetonitrile (ACN). The gel bands were subjected to reduction and alkylation using 5 mM dithiothreitol (DTT) (60°C for 45 min) and alkylation using 10 mM iodoacetamide (IAA). The gel sections were dehydrated with 100% ACN, followed by digestion with trypsin (Gold mass-spectrometry trypsin; Promega, Madison, WI) at 37°C for 10-12 h. The peptides were removed from the gel pieces with 0.4% formic acid in 50% ACN solution and finally with 100% ACN. The extracted peptides were vacuum-dried and stored at – 80°C until LC-MS/MS analysis was undertaken.

LC-MS/MS analysis

The digested samples were acquired by 5600 Triple-TOF mass spectrometer which is directly connected to reverse- phase high-pressure liquid chromatography Ekspert-nanoLC 415 system (Eksigent; Dublin, CA). The trap column (200 μm × 0.5 mm) and the analytical column (75 μm × 15 cm) were both from Eksigent, packed with 3 μm ChromXP C-18 (120 Å) used for reverse phase elution by Ekspert-nano LC 415 system. 0.1% formic acid in water was used as mobile phase A and mobile phase B is 0.1% formic acid in ACN. All fractions were eluted from the analytical column at a flow rate of 250 nL/ min using an initial gradient elution of 10% B from 0 to 5 min, transitioned to 40% over 15 min, ramping up to 90% B for 3 min, holding 90% B for 2 min, followed by re- equilibration of 5% B at 5 min with a total run time of 30 min. Peptides were injected into the mass spectrometer using 10 μm SilicaTip electrospray PicoTip emitter (New Objective Cat. No. FS360-20-10-N-5-C7-CT). Mass spectra (MS) and tandem mass spectra (MS/MS) were recorded in positive-ion and high-sensitivity mode with a resolution of ~35,000 full-width half-maximum. The collected raw files spectra were stored in (dot) .wiff format.

Data analysis

All raw mass spectrometry files were searched in Protein Pilot software v. 5.0.1 (SCIEX) with the Paragon algorithm for relative protein identification. For Paragon searches, the following settings were used: Sample type:

Identification; Cysteine Alkylation: Iodoacetamide, Digestion: Trypsin; Instrument: TripleTOF5600; Species: homosapiens; maximum allowed missed cleavages 1, Search effort: Thorough ID; Results Quality: Correction was automatically applied. The search was conducted using a through identification effort of a Ref-seq database from the National Center for Biotechnology Information (NCBI) website (https://www.ncbi.nlm.nih.gov/refseq/). False discovery rate analysis was also performed through decoy database. Carbamidomethylation (C) was used as a fixed modification. The peptide and product ion tolerance of 0.05 Da was used for searches. The output of this search is a group file and this file contains the following information that is required for targeted data extraction: protein name and accession, cleaved peptide sequence, modified peptide sequence, relative intensity, precursor charge, unused Protscore, confidence, and decoy result.

StavroX 3.6.0.1 analysis

StavroX 3.6.0.1 was chosen as the bioinformatics software [66], as this software is particularly suited for the analysis of intermolecularly crosslinked fragments.

Results and Discussion

Crosslinking details of the 28 kDa 'homodimer' band of lysozyme (14kDa), with the new heterobifunctional crosslinker based on 3HAA

The mass spectral data thus obtained for 28 kDa 'homodimer' band was fed into the StavroX.3.6.0.1 software as a dot (.) .mgf file. As a result, 6784 of 7539 spectra were compared to 166544 theoretical candidates out of which 40135 possible crosslinks were identified within 1 minute and 07 seconds of the run. Major fragments identified by StavroX 3.6.0.1 are shown in Supplementary Figure 11. The software also provided the decoy analysis (Figure 1). "Blue bars represent the number of candidates from the real experimental set, while red bars represent the positive false candidates from the inverted sequence of the FASTA file. More enriched real data set candidates indicate toward better crosslinking". The top ten crosslinked peptide fragments, the intensity of intermolecular crosslinking and efficiency of the crosslinking is shown in Supplementary Figure 12. The highest score for fragment peaks was observed as 116. Figure 2 shows the annotation with the extent of deviation and the identified 'b' and 'y' ions for the fragment m/z 1802.862. "Less deviation in the annotation points toward better crosslinking". The analysis of this peak with the score 105 is shown in Figure 2. Some of the most intense intermolecularly crosslinked peptides according to observed mass as well as specified sequences identified by StavroX 3.6.0.1 are shown in Table 1. For the fragment m/z 1802.862 with the score of 105, "K-6" of Peptide 1 ("LAAAmK") crosslinks via "N-2" of Peptide 2 ("mNAWVAWR"), the major crosslinking site thus being suggested as a link between "K-6" and "N-2"**.** The cross-linked candidate spectrum gives us details about the peptides that are involved in the process of cross-linking also and shows the annotation with the extent of deviation and the identified 'b' and 'y' ions. "Less deviation in the annotation points toward better crosslinking" [The modified fragment ions along with 'b' and 'y' ions, for the highest score 105 with the peak value of m/z 1802.862 is shown in Supplementary Figures 13 and 14].

Crosslinking details of the 38 kDa 'homodimer' band of αA Crystallin (19kDa), with the new heterobifunctional crosslinker based on 3HAA

The mass spectral data thus obtained for 38 kDa 'homodimer' band was fed into the StavroX.3.6.0.1 software as a dot (.) mgf file. As a result, 2935 of 3541 spectra were compared to 157302 theoretical candidates out of which, 35037 possible crosslinks were identified

Citation: Thakur SK, Pal S, Kumar A, Goel R, Eswaran SV (2018) "ESI-MS-Bioinformatics Studies on Crosslinking of αA-Crystallin and Lysozyme using a New Small Aryl Azido-N-HydroxySuccinimidyl Heterobifunctional Crosslinker based on a Metabolite of the Alternative Kynurenine Pathway". J Proteomics Bioinform 11: 192-200. doi: 10.4172/0974-276X.1000486

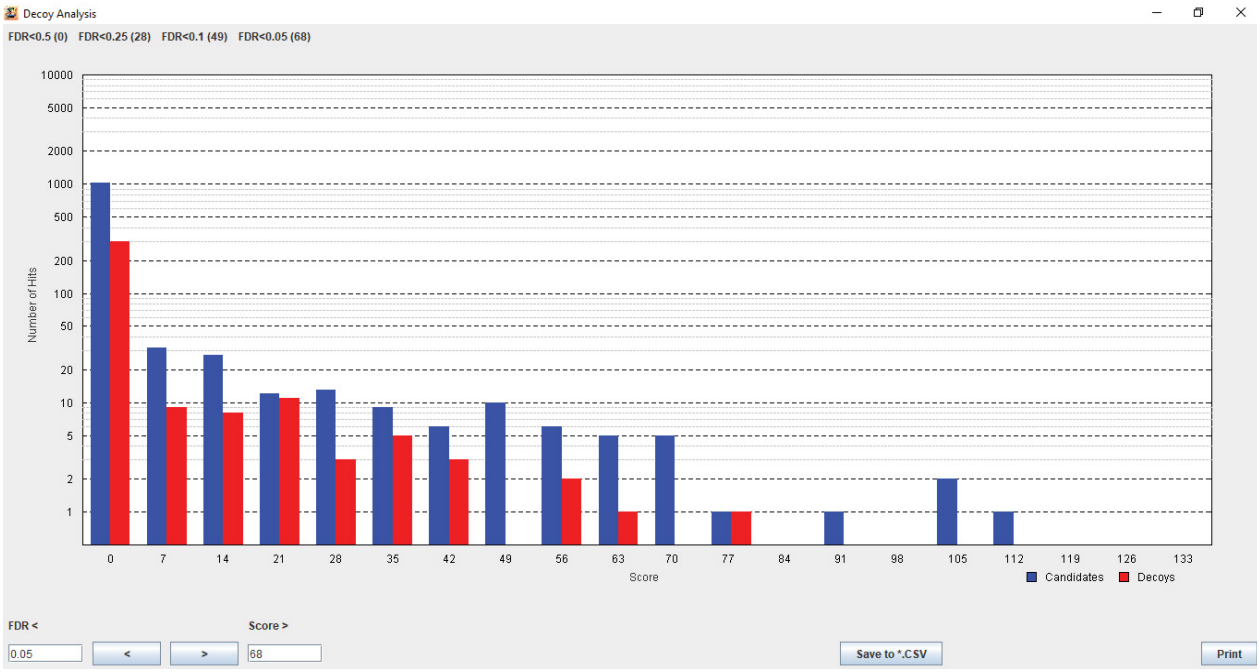

Figure 1: Screen shot of the decoy Analysis for the 28 kDa 'homodimer' band of Lysozyme fragment m/z 1146.540 obtained from StavroX 3.6.0.1. ("Blue bars represent the number of candidates from the real experimental set, while red bars represent the positive false candidates from the inverted sequence of the FASTA file. More enriched real data set candidates indicate toward better crosslinking.").

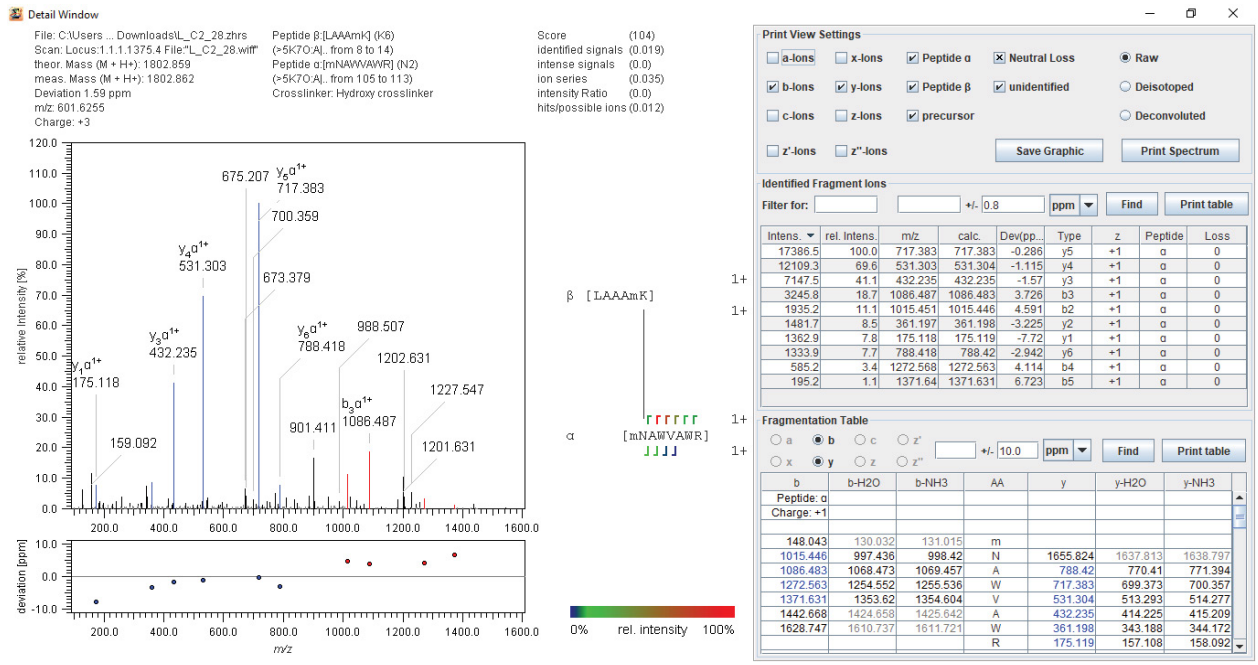

Figure 2: The annotation spectrum with the extent of deviation and identified peaks for the fragment m/z 1802.862 for 28kDa 'homodimer' band obtained from StavroX 3.6.0.1 "Less deviation in the annotation points toward better crosslinking".

Lysozyme with the new heterobifuntional crosslinker	m/z	Peptide 1	Peptide 2	Score	Sequence
Intermolecular cross-linking	1146.540	[KVFG]	[BELAA]	116	K1-A5+CXL
	1802.862	[LAAAmK]	[mNAWVAWR]	105	K6-N2+CXL
	1854.860	[TPGSRN]	[GMNAWVAWR]]	77	S4-W5+CXL
	1655.821	[ELAAAMK]	[KIVSDGNG]	74	E1-S4+CXL

Table 1: The intermolecularly crosslinked fragments with high scores identified by the software.

within 1 minute and 16 seconds of the run. Major fragments identified by StavroX 3.6.0.1 is shown in Supplementary Figure 15. The software also provided the decoy analysis (Figure 3). As stated above, "Blue bars represent the number of candidates from the real experimental set, while red bars represent the positive false candidates from the inverted sequence of the FASTA file. More enriched real data set candidates indicate toward better crosslinking". The top ten crosslinked peptide fragments, the intensity of intermolecular crosslinking and efficiency of the crosslinking is shown in Supplementary Figure 16. The highest score for fragment peaks was observed as 66. Figure 4 shows the annotation with the extent of deviation and the identified 'b' and 'y' ion for the fragment m/z 1286.540. "Less deviation in the annotation points toward better crosslinking" The analysis of this peak with the score 66 is shown in Figure 4. Some of the most intense intermolecularly crosslinked peptides according to observed mass as well as specified sequences identified by StavroX 3.6.0.1 are shown in Table 2. For the fragment m/z 1286.640 with the score of 66, "S-1" of Peptide 1 ("SAPSS") crosslinks via "D-5" of Peptide 2 ("VIFLDV"), the major crosslinking site thus being suggested as a link between "S-1" and "D-5". The cross-linked candidate spectrum gives us details about the peptides that are involved in the process of cross-linking, the annotation with the extent of deviation and the identified 'b' and 'y' ions. The modified fragment ions along with 'b' and 'y' ions, for the highest score 66 with the peak value of m/z 1286.640 is shown in Supplementary Figure 17.

Crosslinking details of the 33 kDa 'heterodimer' band of αA-Crystallin (19kDa) and lysozyme (14kDa), with the new heterobifunctional crosslinker based on 3HAA

The mass spectral data thus obtained for 33 kDa 'heterodimer' band was fed into the StavroX.3.0.6.1 software as a dot (.) mgf file. As a result, 2011 of 2012 spectra were compared to 14460479 theoretical candidates out of which, 1759 possible crosslinks were identified within 1 minute and 02 seconds of the run. Major fragments identified by StavroX3.6.0.1 are shown in Supplementary Figure 18. The software also provided the decoy analysis (Figure 5). As stated above, "Blue bars represent the number of candidates from the real experimental set, while red bars represent the positive false candidates from the inverted sequence of the FASTA file. More enriched real data set candidates indicate toward better crosslinking". The top ten crosslinked peptide fragments, the intensity of intermolecular crosslinking and efficiency of the crosslinking is shown in Table 3. The highest score for fragment peaks was observed as 86. Figure 6 shows the annotation with the extent of deviation and the identified 'b' and 'y' ion for the fragment m/z1290.597. "Less deviation in the annotation points toward better crosslinking". The analysis of this peak with the score 86 is shown Figure 6. Some of the most intense intermolecularly crosslinked peptides according to observed mass as well specified sequence identified by StavroX 3.6.0.1 are shown in Table 4. A most significant intermolecularly crosslinked fragment with a peptide each from αA-Crystallin and from Lysozyme was observed with the value of m/z 1290.597. For this fragment with m/z 1290.597 and the score of 86, "S-1" of Peptide 1 ("SALSB") crosslinks via "L-1" of Peptide 2 ("LAAAmK"), the major crosslinking site thus being suggested as a link between "S-1" and "L-1". The cross-linked candidate spectrum. Figure 7 gives the details about the peptides that are involved in the process of cross-linking and also shows the annotation with the extent of deviation and the identified 'b' and 'y' ions. The modified fragment ions along with 'b' and 'y' ions, for the highest score 86 with the peak value of m/z 1290.597 is shown in Supplementary Figure 19. Additional experiments done, using reduced lysozyme, mutant αA-Crystallin and with lysozyme and αA-Crystallin using the crosslinker (ATFB, SE) are included in Supplementary Figures 19-22 as these did not give significant results.

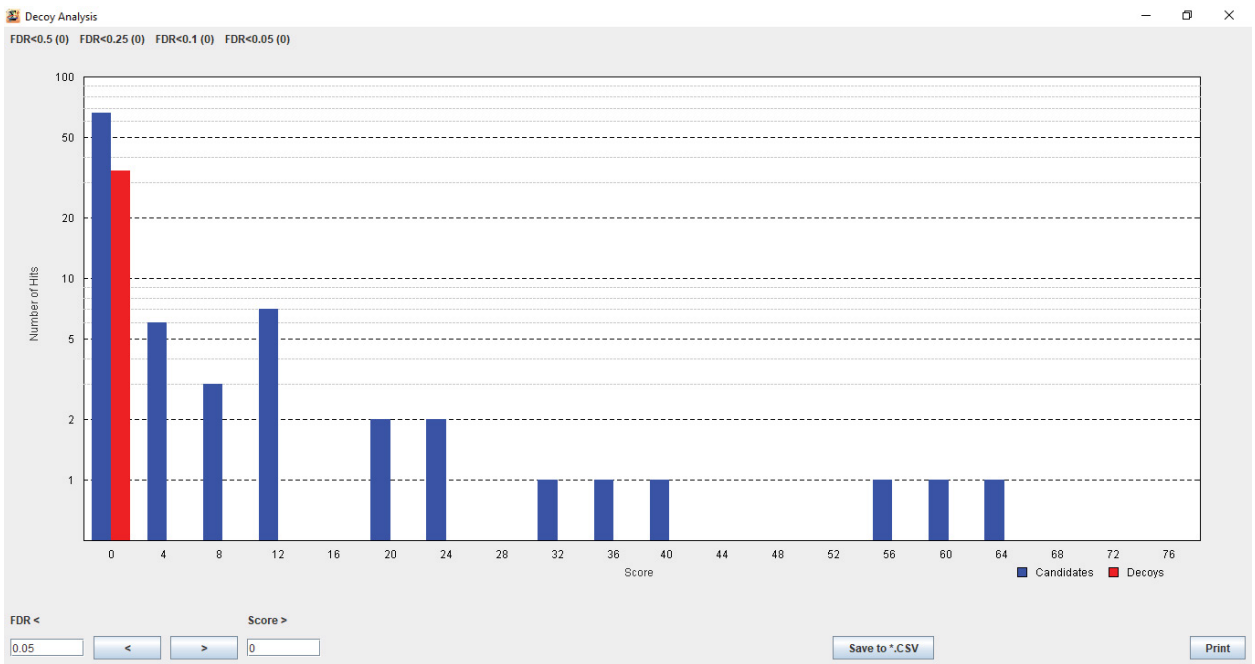

Figure 3: Screen shot of the decoy Analysis for the 38 kDa 'homodimer' band of αA-Crystallin fragment m/z 1286.540 obtained from StavroX 3.6.0.1. ("Blue bars represent the number of candidates from the real experimental set, while red bars represent the positive false candidates from the inverted sequence of the FASTA file. More enriched real data set candidates indicate toward better crosslinking.").

Citation: Thakur SK, Pal S, Kumar A, Goel R, Eswaran SV (2018) "ESI-MS-Bioinformatics Studies on Crosslinking of αA-Crystallin and Lysozyme using a New Small Aryl Azido-N-HydroxySuccinimidyl Heterobifunctional Crosslinker based on a Metabolite of the Alternative Kynurenine Pathway". J Proteomics Bioinform 11: 192-200. doi: 10.4172/0974-276X.1000486

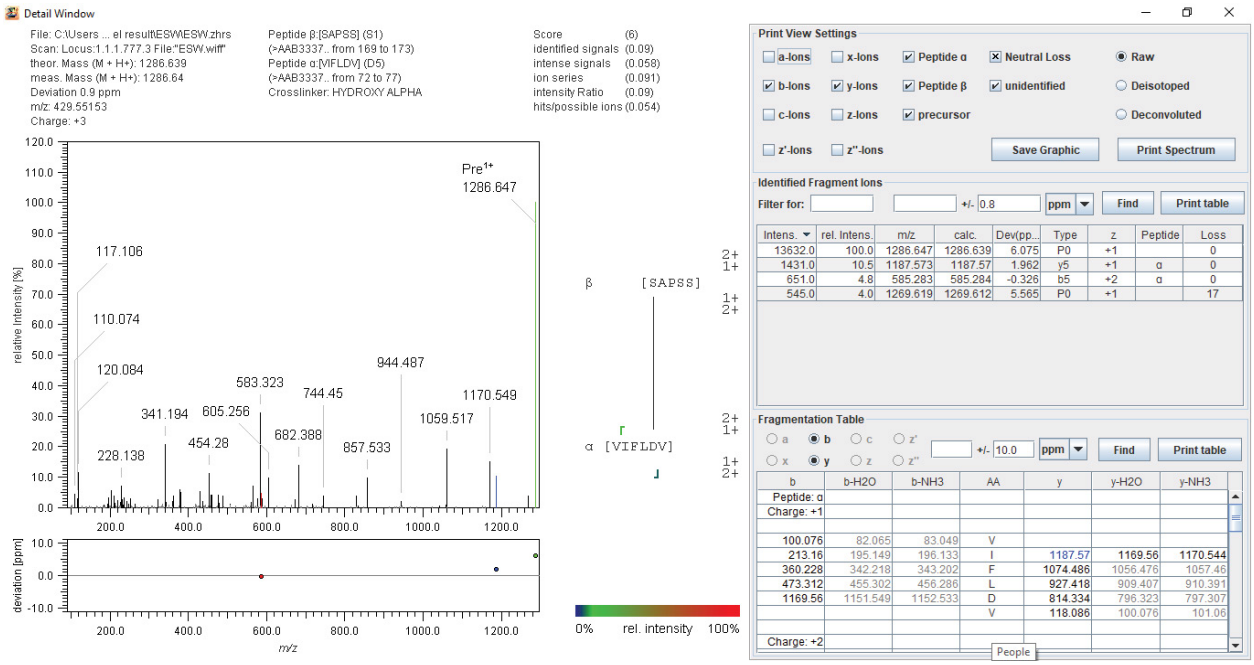

Figure 4: The annotation spectrum with the extent of deviation and identified peaks for the fragment m/z 1286.640 of 38kDa 'homodimer' band of αA-Crystallin obtained from StavroX 3.6.0.1. "Less deviation in the annotation points toward better crosslinking".

αA-Crystallin with the new heterobifunctional crosslinker	m/z	Peptide 1	Peptide 2	Score	Sequence
Intermolecular Cross-linking	1286.640	[SAPSS]	[VIFLDV]	66	S1-D5+CXL
	1286.640	[VLDSG]	[LPFLSS]	63	L2-S6+CXL
	2173.153	[RRYRLP]	[DATHAERAIPV]	61	Y3-L2+CXL
	1417.692	[GKHNE]	[IPVSRE]	56	K2-P2+CXL
	2173.153	[VIFLDV]	LTFBGPKIQT]	54	D5-K7+CXL

Table 2: The intermolecularly crosslinked fragments with high scores identified by the software.

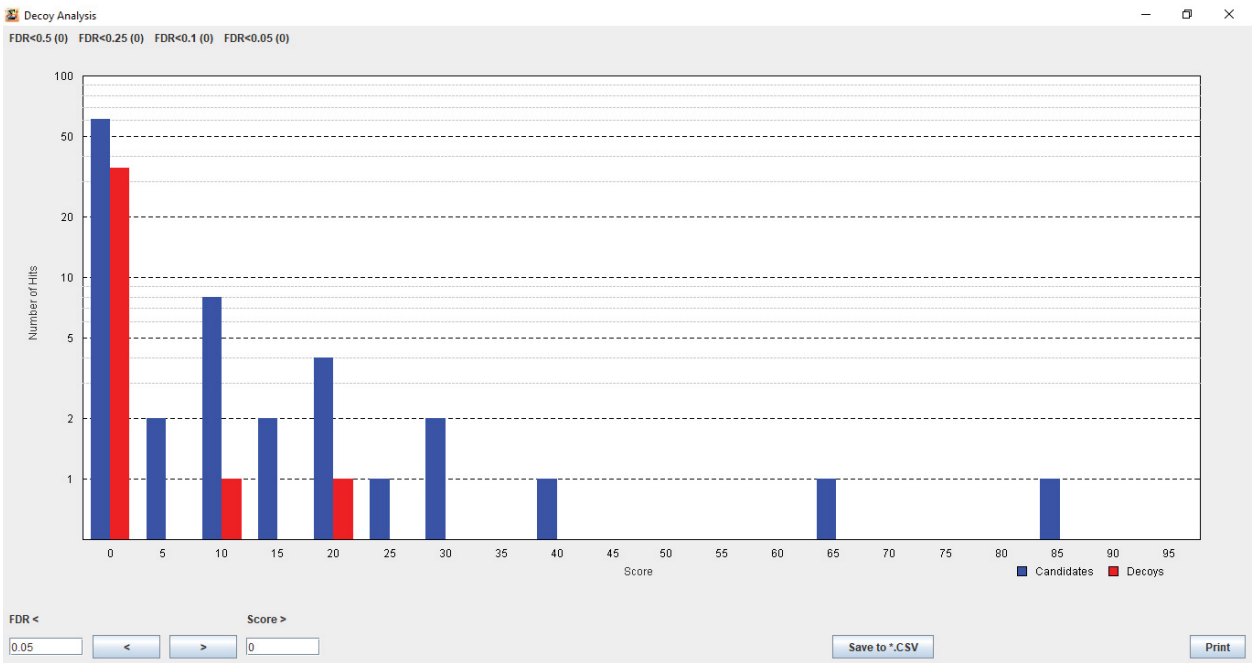

Figure 5: Screen shot of the decoy Analysis for the 33 kDa 'heterodimer' band of αA-Crystallin and lysozyme fragment m/z 1290.597 obtained from StavroX 3.6.0.1. ("Blue bars represent the number of candidates from the real experimental set, while red bars represent the positive false candidates from the inverted sequence of the FASTA file. More enriched real data set candidates indicate toward better crosslinking.").

Citation: Thakur SK, Pal S, Kumar A, Goel R, Eswaran SV (2018) "ESI-MS-Bioinformatics Studies on Crosslinking of αA-Crystallin and Lysozyme using a New Small Aryl Azido-N-HydroxySuccinimidyl Heterobifunctional Crosslinker based on a Metabolite of the Alternative Kynurenine Pathway". J Proteomics Bioinform 11: 192-200. doi: 10.4172/0974-276X.1000486

Nr.	Score	m/z	z	M+H+	calc.	Dev(...	Peptide(1)	Protein (1)	From(...	To(1)	Peptide(2)	Protein (2)	From(...	To(2)	Site(1)	Site(2)	Rank	Scan	RT
1	86	645.802	2	1290.597	1290.594	2.22	[SALSB]	SALLSSDITAS....	67	71	[LAAAmK]	>5K70:A|PDBI....	8	13	S1	L1	1	Locus:1.1.....	1328
2	68	410.518	3	1229.539	1229.541	-1.2	[SLSAD]	SALLSSDITAS....	72	76	[KVQDD]	SALLSSDITAS....	28	32	S3	Q3	1	Locus:1.1.....	1362
3	67	410.518	3	1229.539	1229.541	-1.2	[SLSAD]	SALLSSDITAS....	72	76	[IVSDGN]	SALLSSDITAS....	116	121	S3	V2	2	Locus:1.1.....	1362
4	67	410.518	3	1229.539	1229.541	-1.2	[SLSAD]	SALLSSDITAS....	72	76	[QTDLGA]	SALLSSDITAS....	87	92	S3	T2	3	Locus:1.1.....	1362
5	42	410.518	3	1229.539	1229.541	-1.2	[TGLDA]	SALLSSDITAS....	88	92	[DQSALS]	SALLSSDITAS....	65	70	L3	S3	4	Locus:1.1.....	1362
6	42	681.34	3	2042.006	2042.008	-0.88	[NGMNAW]	SALLSSDITAS....	121	127	[VIFLDVKHF]	SALLSSDITAS....	12	20	V7	K7	1	Locus:1.1.....	1516
7	37	410.518	3	1229.539	1229.541	-1.2	[GLDAT]	SALLSSDITAS....	89	93	[DQSALS]	SALLSSDITAS....	65	70	T5	D1	5	Locus:1.1.....	1362
8	32	737.708	3	2211.11	2211.11	-0.49	[ELAAAmKR]	>5K70:A|PDBI....	7	14	[NAWVAWRNR]	SALLSSDITAS....	124	132	K7	N8		Locus:1.1.....	1626
9	30	645.802	2	1290.597	1290.594	2.22	[ALSBS]	SALLSSDITAS....	68	72	[LAAAmK]	>5K70:A|PDBI....	8	13	A1	K6	2	Locus:1.1.....	1328
10	30	410.518	3	1229.539	1229.541	-1.2	[SLSAD]	SALLSSDITAS....	72	76	[IVSDGN]	SALLSSDITAS....	116	121	S3	|1	1	Locus:1.1.....	1369

Table 3: Top ten intermolecularly crosslinked fragments as given by software StavroX 3.6.0.1.

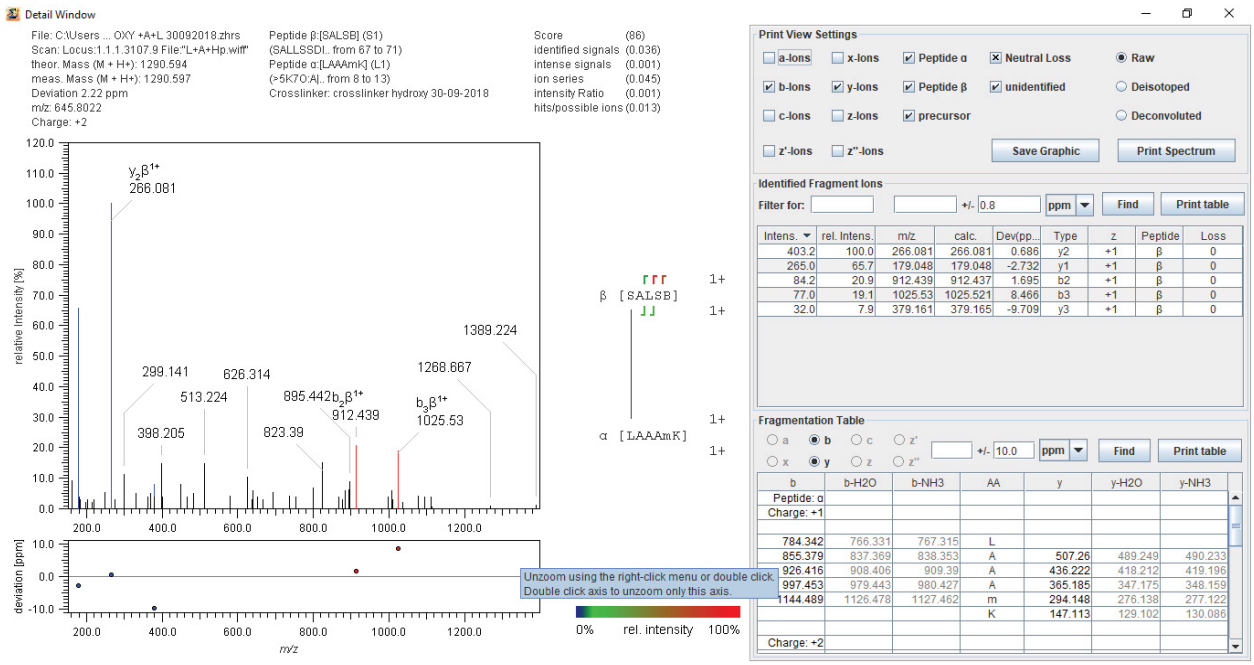

Figure 6: The annotation spectrum with the extent of deviation and identified peaks for the fragment m/z 1290.597 of the 33 kDa 'heterodimer' band of αA-Crystallin and lysozyme obtained from StavroX 3.6.0.1. "Less deviation in the annotation points toward better crosslinking".

αA-Crystallin and Lysozyme with new heterobifunctional crosslinker	m/z	Peptide 1	Peptide 2	Score	Sequence
Intermolecular Crosslinking	1290.597	[SALSB]	[LAAAmK]	86	S1-L1+CXL
	1229.539	[SLSAD]	[IVSDNG]	67	S3-V2+CXL
	2042.006	[NGMNAWV]	[VIFLDVKHF]	42	A5-K7+CXL
	1290.597	[ALSCS]	[LAAAmK]	30	A1-K6+CXL
	1229.539	[SLSAD]	[IVSDGN]	30	S3-I1+CXL

Table 4: The intermolecularly crosslinked fragments with high scores identified by the software.

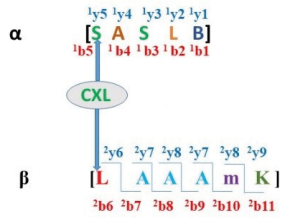

Figure 7: The intermolecular crosslinking sites in the peptide fragments m/z 1290.597 along with the 'b' and 'y' ions obtained from StavroX 3.6.0.1 Software. This most significant intermolecularly crosslinked fragment contains a peptide fragment each from αA-Crystallin and from Lysozyme. The peptide fragments identified are in the ACD region and thus could be important for understanding the chaperoning mechanism of αA-Crystallin and cataractogensis.

Conclusion

α-Crystallins have become important not only for understanding diseases of the human eye but are also being considered as therapeutics for treatment of other diseases. Instead of the whole protein the Alpha Crystallin Domain (ACD) or Mini Alpha-crystallin Chaperons (MACs) could themselves serve as therapeutics. These ACDs are conserved across most HSPs. It is thus important to understand the role of Crystallins in chaperoning mechanism and treatment/ cure and onset of other diseases. Crosslinking studies on αA-Crystallin have been carried out previously. However, most of these studies were restricted to use of homobifunctional crosslinkers, which could not elicit as much information about intermolecular crosslinking. The work described here deals with crosslinking of lysozyme, αA-Crystallin, and a 1:1 mixture of αA-Crsytallin and lysozyme, using a small Aryl

Azido-N-hydroxy succinimide (NHS) heterobifunctional crosslinker. Using a two-step protocol, i. e. an initial incubation step followed by photolysis (366 nm, 6W UV lamp), SDS-PAGE, excision of 'homo and hetero Dimer' bands, trypsinization, ESI- MS, MS/MS investigations and analysis of the MS data using StavroX 3.6.0.1, a bioinformatics software especially suited for identifying intermolecular crosslinking. Our results have identified many significant intermolecular crosslinks not previously identified. Many of these are in the ACD region and thus could be important for understanding the chaperoning mechanism of αA-Crystallin and cataractogensis. The new crosslinker could also find application for treating keratoconus, a disease affecting the human cornea [67].

Acknowledgement

Authors thank Dr Sudhanshu Vrati, Executive Director, Regional Centre for Biotechnology (RCB) Faridabad, Haryana, India and Dr Gagandeep Kang, Executive Director, Translational Health Science and Technology Institute (THSTI), Faridabad, Haryana, India for research facilities and AcSIR for Emertius Professorship (Hony.) (to SVE). We thank the Advanced Technology Platform Center (ATPC, RCB) & Dr. Nirpender Singh for his advice and for supervising the ESI-MS, MS/MS studies. We thank Dr. Krishna Sharma, University of Missouri–Columbia School of Medicine, Columbia, Missouri, USA for providing us mutant G98R αA- Crystallin. We are grateful to Prof Vani Bramhachari (Dr. B.R. Ambedkar Centre for Biomedical Research (ACBR), Delhi University) for help with initial experiments, Dr. D Balasubramanian, (Director, Research, at LV Prasad Eye Institute, Hyderabad), for encouragement. We thank Dr Ch. Mohan Rao (Centre for Cellular & Molecular Biology, Hyderabad) for providing us cloned αA-Crystallin. We thank, Dr. Michael Goetze University of Halle-Salle, Germany for providing the StavroX 3. 6.0.1 software. One of us (RG) thanks THSTI for intramural core grant for funding.

Conflict of Interest

The authors have no conflict of interest to declare.

Author Contributions

SVE conceptualized the problem, S.K.T. & S.V.E. did synthesis, characterization, incubation-photolysis; A.K. & R.G. did SDS-PAGE and ESI-MS; M.S. S.K.T. & S.V.E. did StavroX 3.6. 0.1 software; S.V.E., R.G. wrote the paper & S.K.T. helped in compilation.

References

1. Horwitz J (1992) Alpha-Crystallin can function as a molecular Chaperone. Proc Natl Acad 89: 10449-10453.
2. Nagaraj RH, Nahomi RB, Mueller NH, Raghavan CT, Ammar DA, et al. (2016) Therapeutic Potential of α-Crystallin, Biochim Biophys Acta 1860: 252-257.
3. Nagaraj RH, Linetsky M, Stitt AW (2012) The pathogenic role of Maillard reaction in the aging eye. Amino Acid 42: 1205-1220.
4. Nargaraj RH, Oya-Ito T, Padayatti PS, Kumar R, Mehta S, et al. (2003) Enhancement of chaperone function of alpha crystallin by methylglyoxal modification. Biochemistry 42: 10746-10755.
5. Nagraj RH, Panda AK, Shanthakumar S, Santhoshkumar P, Pasupuleti N, et al. (2012) Hydroimidazolone modification of the conserved Arg12 in small heat shock proteins: studies on the structure and chaperone function using mutant mimics. PLoS One 7: e30257.
6. Puttiah S, Biswas A, Staniszewska M, Nagaraj RH (2007) Methylglyoxal inhibits glycation-mediated loss in chaperone function and synthesis of pentosidine in alpha- crystalline. Exp Eye Res 84: 914-921.
7. Nagaraj RH, Nahomi RB, Shanthakumar S, Linetsky M, Padmanabha S, et al. (2012) Acetylation of αA-crystallin in the human lens: effects on structure and chaperone function. Biochim Biophys Acta 822: 120-129.
8. Nahomi RB, Huang R, Nandi SK, Wang B, Padmanabha S, et al. (2013) Acetylation of lysine 92 improves the chaperone and anti-apoptotic activities of human αB-crystallin. Biochemistry 52: 8126-8138.
9. Pasupuleti N, Matsuyama S, Voss O, Doseff AI, Song K, et al. (2010) The anti-apoptotic function of human αA-crystallin is directly related to its chaperone activity. Cell Death Dis: e31.
10. Forta PE, Lampi KJ (2011) New focus on alpha-crystallins in retinal neurodegenerative diseases. Exp Eye Res 92: 98-103.
11. Darlington LG, Forrest CM, Mackay GM, Smith RA, Smith AJ, et al. (2010) On the Biological importance of the 3-hydroxyanthranilic Acid: Anthanilic acid ratio. Int J Tryptophan Res 3: 51-59.
12. Korlimbinis A, Hains PG, Truscott JW, Aquilina JA (2006) 3-Hydroxykynurenine oxidises αA-Crystallin: Potential role in cataractogenisis. Biochemistry 45: 1852-1860.
13. Goldstein LE, Leopold MC, Huang X, Atwood CS, Saunders AJ, et al. (2000) 3-hydroxykynurenine and 3-hydroxyanthranilic acid generate hydrogen peroxide and permote α-Crystallin cross-linking by Metal Ion Reduction. Biochemistry 39: 7266-7275.
14. Srivastava OP, Kirk MC, Srivastava K (2004) Characterization of Covalent Multimers of Crystallins in Aging Human Lenses. J Biol Chem 279: 10901-10909.
15. Gupta R, Srivastava OP (2009) Identification of interaction sites between human betaA3- and alphaA/ alphaB-crystallins by mammalian two-hybrid and fluorescence resonance energy transfer acceptor photobleaching methods. J Biol Chem 284: 18481-18492.
16. Shridas P, Sharma Y, Balasubramanian D (2001) Transglutaminase–mediated cross-linking of alpha-crystallin: structural and functional consequences FEBS Letters 499: 245-250.
17. Kanwar R, Balasubramainian D (1999) Structure and stability of the dityrosine-linked Dimer of γB-crystalin. Exp Eye Res 68: 773-784.
18. Raman B, Ramakrishna T, Rao CM (1997) (Effect of the chaperone-like alpha-crystallin on the refolding of lysozyme and ribonuclease A. FEBS Letters 416: 369-372.
19. Raman B, Rao CM (1994) Chaperone-like activity and quaternary structure of alpha-crystallin. J Biol Chem 269: 27264-27268.
20. (a) Peschek J, Braun N, Franzmann TM, Georgalis Y, Haslbeck M, et al. (2009) The eye lens chaperone α-crystallin forms defined globular assemblies, Proc Natl Acad 106: 13272-13277. 20 (b) Abgar S, Vanhoudt J, Aerts T, Clauwaert J (2001) Study of the Chaperoning Mechanism of Bovine Lens α-Crystallin, a Member of the α-Small Heat Shock Superfamily. Biophysical J 80: 1986-1995.
21. Sharma KK, Kumar RS, Kumar GS, Quinin PT (2000) Synthesis and characterization of a peptide identified as a functional element in alphaA-crystallin. J Biol Chem 275: 3767-3771.
22. Bhattacharyya J, Udupa EGP, Wang J, Sharma KK (2006) (Mini-alpha B crystallin: a functional element of alpha B-crystallin with chaperone-like activity. Biochemistry 45: 3069-3076.
23. Santhoshkumar P, Sharma KK (2002) Identification of a region in alcohol dehydrogenase that binds to alpha-crystallin during chaperone action. Biochim Biophys Acta 1598: 115-121.
24. Kannan R, Santhosh kumar P, Mooney BP, Sharma KK (2013) The αA66-80 peptide interacts with soluble alpha-crystallin and induces its aggregation and precipitation: a contribution to age-related cataract formation. Biochemistry 52: 3638-3650.
25. Gosh JG, Houck SA, Clark JI (2007) Interactive sequences in the stress protein and molecular chaperone human alphaBcrystallin recognize and modulate the assembly of filaments. Int J Biochem Cell Biol 39: 1804-1815.
26. Fukuhara S, Nishigaki T, Miyata K, Tsuchiya N, Waku T, et al. (2012) Mechanism of the chaperone-like and antichaperone activities of amyloid fibrils of peptides from alpha A-crystallin. Biochemistry 51: 5394-5401.
27. Houck SA, Landsbury L, Clark JI, Quinlan RA (2011) Multiple sites in alpha B-crystallin modulate its interactions with desmin filaments assembled in vitro. PLoS One 6: e25859.
28. Hoffman A, Bukau B, Kramer G (2010) Structure and function of the molecular chaperone trigger factor. Biochim Biophys Acta 1803: 650-661.

29. Fischer L, Chen ZA, Rappsilber J (2013) Quantitative cross-linking/mass spectrometry using isotope-labelled cross-linkers. J Proteomics 88: 120-128.

30. Sutherland BW, Toews J, Kast J (2008) Utility of formaldehyde cross□linking and mass spectrometry in the study of protein–protein interactions. J Mass Spectrom 43: 699 -715.

31. Rappsilber J (2011) The beginning of a beautiful friendship: cross-linking/mass spectrometry and modelling of proteins and multi-protein complexes. J Struct Biol 173: 530-540.

32. Holding AN (2015) XL-MS: Protein cross-linking coupled with mass spectrometry. Methods 8: 54-63.

33. Cravatt BF, Gabriel MS, John RY, Iii JR (2007) The biological impact of mass-spectrometry-based proteomics. Nature 450: 991-1000.

34. Schmidt C, Urlaub H (2017) Combining cryo-electron microscopy (cryo-EM) and cross-linking mass spectrometry (CX-MS) for structural elucidation of large protein assemblies. Curr Opin Struc Biol 46: 157-168.

35. Zabailov BL, Glazko GV, Jaiswal M, Raney KD (2013) Large Scale Chemical Cross-linking Mass Spectrometry Perspectives. J Proteomics Bioinform S2: 001.

36. Courcelles M, Coulombe HJ, Cossette E, Gingras A, Thibault P, et al. (2017) CLMSVault: a software suite for protein cross-linking mass spectrometry data analysis and visualization. J Proteome Res 6: 2645-2652.

37. Kosinski J, VonAppen A, Ori A, Karius K, Muller C, et al. (2015) Xlink analyzer: software for analysis and visualization of cross-linking data in the context of three-dimensional structures. J Struct Biol 189: 177-183.

38. Rinner O, Seebacher J, Waltzthoeni T, Muller LN, Beck M, et al. (2008) Identification of cross-linked peptides from large sequence databases. Nat Methods 5: 315-318.

39. Russel D, Lasker K, Webb B, Tjioe E, Peterson B, et al. (2012) Putting the Pieces Together: Integrative Modeling Platform Software for Structure Determination of Macromolecular Assemblies. PLOS Biol: e1001244.

40. Bayley H (1983) Photogenerated Reagent in Biochemistry and Molecular Biology. Laboratory Techniques in Biochemistry and Molecular Biology. Elsevier Science.

41. Platz MS (1989) Comparison of Phenylcarbene and Phenylnitrene. Acc Chem Res 28: 487-492.

42. Platz MS, Kanakarajan K, Goodrich RP, Young MJT, Soundararajan S, et al. (1988) Spectroscopy of Nitrenes bound to α-Chymotrypsin Proceedings. New direction in Photodynamic Thearpy: 487.

43. Tomioka H, Ichikawa N, Kamatsu K (1993) Photochemistry of 2-(methoxycarbonyl) phenyl azide studied by matrix-isolation spectroscopy. A new slippery energy surface for phenylnitrene. J Am Chem Soc 115: 8621-8626.

44. Borden WT, Gritsan NP, Hadad CM, Karney WL, Kemnitz CR, et al. (2000) The interplay of theory and experiment in the study of phenylnitrene. Acc Chem Res 33: 765-771.

45. Xue J, Luk LH, Eswaran SV, Platz MS, Hadad CM, et al. (2012) Ultrafast Infrared and UV-vis Studies of the Photochemistry of 2-Methoxy-6-Methoxycarbonylphenyl Azide in Solution. J Phys Chem 116: 5325-5336.

46. Thakur KS, Eswaran SV (2017) A New Hetero Cross-linker Based On an "Introverted" Acid: Mass Spectrometry and Bioinformatics Studies, Analysis of Intermolecular Crosslinking of Proteins. J Anal Bioanal Tech 8: 393.

47. Thakur KS, Eswaran SV (2018) ESI-MS and Stavrox 3.6.0.1 Investigations of Crosslinking by an Aryl-Azido-NHSHeterobifunctionalCrosslinker. J Anal Bioanal Tech 9.

48. Pal S, Ganesan K, Eswaran SV (2018) Chemical Crosslinking-Mass spectrometry (CXL-MS) for Proteomics, Antibody-Drug conjugates (ADCs) and Cryo-Electron Microscopy (cryo-EM). IUBMB Life 70: 947-960.

49. Kaur D, Luk HL, Coldren W, Srinivas MP, Lakshetti S, et al. (2014) Concomitant Nitrene and Carbene Insertion Accompanying Ring Expansion: Spectroscopic, X-ray and Computational Studies. J Org Chem 79: 1199-1205.

50. Eswaran SV, Kaur D, Khamaru K, Prabhakar S, Sony T, et al. (2016) Tuning the strain effect to induce selectivity through intramolecular nitrene insertion into an adjacent methoxy C H bond leading to form a new benzoxazole: experimental and computational studies. Tetrahedron Letters 57: 1899-1902.

51. Eswaran SV, Kaur D, Jana K, Khamaru K, Prabhakar S, et al. (2017) Nitrene insertion into an adjacent o-methoxy group followed by nucleophilic addition to the heterocumulene intermediate: Experimental and computational studies. Tetrahedron 73: 5280-5288.

52. Goswami M, Lyaskovskyy V, Domingost SR, Buma WJ (2015) Characterization of Porphyrin-Co(III)- 'Nitrene Radical' Species Relevant in Catalytic Nitrene Transfer Reaction. J Am Chem Soc 137: 5468-5479.

53. Sinz A, Arlt C, Chorev D, Sharon M (2015) Chemical cross-linkingand native mass spectrometry: a fruitful combination for structural biology. Protein Sci 24: 1193-1209.

54. Sinz A (2014) The advancement of chemical cross-linking and mass spectrometry for structural proteomics: from single proteins to protein interaction networks." Expert Rev Proteomics 11: 733-743.

55. Stengel F, Aebersold R, Robinson CV (2012) Joining Forces: Integrating Proteomics and Cross-linking with the Mass Spectrometry of Intact Complexes. Mol Cell Proteomics 11: R111.014027.

56. Hermanson GT (2008) Bioconjugate Techniques IIndEdn, Acadmic Press. New York.

57. Ewens CA, Panico S, Kloppesteck P, Mckeown C, Robinson C, et al. (2014) The p97-FAF1 protein complex reveals a common mode of p97 adaptor binding. J Biol Chem 289: 12077-12084.

58. Leitner A, Faini M, Stengel F, Aebersold R (2016) Crosslinking and Mass Spectrometry: An Integrated Technology to Understand the Structure and Function of Molecular Machines. Trends in Biochem Sci 41: 20-32.

59. Walzthoeni T, Joachimaik LA, Rosenberger G, Röst HL, Malmström L, et al. (2015) xTract: software for characterizing conformational changes of protein complexes by quantitative cross-linking mass spectrometry. Nature Methods 12: 1185-1190.

60. Dihazi GH, Sinz A (2003) Mapping low-resolution three-dimensional protein structures using chemical cross-linking and Fourier transform ion-cyclotron resonance mass spectrometry. Rapid Commun Mass Spectrom 17: 2005-2014.

61. Back JW, Sanz MA, DeJong L, De Konning LJ, Nijtmans LGJ, et al. (2002) A structure for the yeast prohibition complex: Structure prediction and evidence from chemical crosslinking and mass spectrometry. Protein Science 11: 2471-2478.

62. Ehresmann C, Moine H, Mougel M, Dondon J, Ehresmann B, et al. (1986) "Cross-linking of initiation factor IF3 to Escherichia coli 30S ribosomal subunit by trans-dlamminedichloroplatinum (II): characterization of two cross-linking sites in 16S rRNA; a possible way of functioning for IF3. Nucleic Acids Res 14: 4803-4821.

63. Fritzsche R, Ihling Ch, Gotze M, Sinz A (2012) Optimizing the enrichment of crosslinked products for mass spectrometric protein analysis. Rapid Commun Mass Spectrom 26: 653-658.

64. Kao A, Chiu CL, Vellucci D, Yang Y, Patel VR, et al. (2010) Development of a novel cross-linking strategy for fast and accurate identification of cross-linked peptides of protein complexes. Mol Cell Proteomics 10: M110.002212.

65. Goel R, Murthy KR, Srikanth SM (2013) A Characterizing the normal proteome of human ciliary body. Cilin Proteomics 10: 9.

66. Gotze M, Pettelkau J, Fritzsche R, Ihling CH, Schafer M, et al. (2014) Automated assignment of MS/MS cleavable cross-links in protein 3D-structure analysis. J Am Soc Mass Spectrom 26: 83-97.

67. "Crosslinker for karetoconus" https://www.youtube.com/watch?v=sQHfDWgEhQs